Characterization of Large, Polyanionic Inorganic Molecules: Fast Atom Bombardment Mass Spectrometry of $P_2W_{15}Nb_3O_{62}^{9-}$ and of the Supported Organometallic Catalyst Precursor $(1,5\text{-COD})Ir{\cdot}P_2W_{15}Nb_3O_{62}^{8-}$

Alessandro Trovarelli[†] and Richard G. Finke*[‡]

Department of Chemistry, University of Oregon, Eugene, Oregon 97403

Received March 31, 1993[⊗]

Positive and negative ion FAB-MS (fast atom bombardment mass spectrometry) has been used to help characterize large polyoxoanions with molecular weights of up to 6300 mass units, specifically $[Bu_4N]_9P_2W_{15}Nb_3O_{62}$ and the important polyoxoanion-supported iridium organometallic complex $[Bu_4N]_5Na_3[(1,5\text{-COD})Ir{\cdot}P_2W_{15}Nb_3O_{62}]$. A detailed assignment of more than 50 envelopes has been performed, including the comparison of experimental vs calculated molecular ion distributions for key fragments. Two main pathways account for the most common fragmentations in both positive and negative ion FAB-MS, the loss of WO_3 and the loss of O (and/or H_2O, the latter generally following cation exchange between H^+ from the matrix and Bu_4N^+ or Na^+). The excellent agreement between the experimental and calculated isotopic ion distributions provides reliable molecular formulas, even for fragments differing by only a few mass units. A higher degree of fragmentation is observed in the negative ion mode; this provides interesting structural and mechanistic results, notably the formation of a "$P_2W_{10}Nb_2O_{42}^{4-}$" fragment analogous to the "P_2W_{12}" polyoxoanion described in the literature. Overall, the most important finding is that most of the peaks in such complicated mass spectra can be readily assigned in terms of simple mechanisms and now-established polyoxoanion-fragmentation chemistry.

Introduction

Polyoxoanion chemistry has continued to expand significantly over the past decade primarily due to three reasons: the fundamental interest in this large class of inorganic complexes, the wide range of known and potential applications of polyoxoanions, and the concurrent development of powerful physical tools such as rapid X-ray diffraction structural analysis or ^{183}W NMR spectroscopy.[1] However, the unambiguous and especially the *more rapid* characterization of polyoxoanions is still problematic in some instances such as for organic-solvent soluble salts of polyoxoanions.[2] For example, X-ray crystallography is currently virtually useless for organic solvent-soluble salts of larger, more polycharged polyoxoanions due to the difficulties in obtaining suitably diffracting crystals for such nonaqueous soluble systems. Hence any development or application of modern physical methods that proves to be rapid and effective for characterization of the polyoxoanions and their derivatives, such as our initial[3] and now the present work with fast atom bombardment mass spectrometry (FAB-MS) as well as the important efforts of others,[4] is significant.

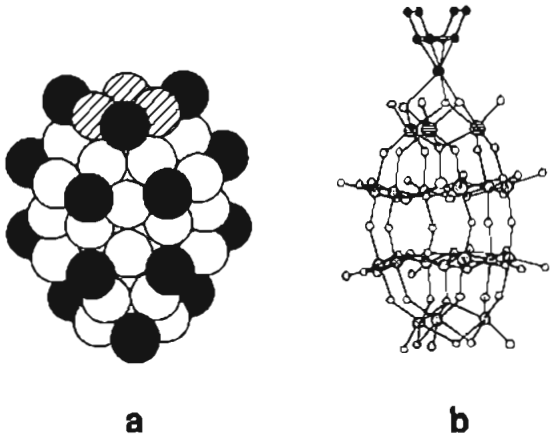

Figure 1. Space-filling representation of $P_2W_{15}Nb_3O_{62}^{9-}$ and ball and stick model of the proposed structure of $(Bu_4N)_5Na_3[(1,5\text{-COD})Ir{\cdot}P_2W_{15}Nb_3O_{62}]$.[2d] In the space-filling model the hatched circles are Nb–O–Nb oxygens, the gray circles terminal Nb–O oxygens, and the white and black circles bridging and terminal oxygens, respectively.

Herein we report the use of FAB-MS to help rapidly characterize the massive and highly charged polyoxoanion $P_2W_{15}Nb_3O_{62}^{9-}$ and its supported-organometallic derivative $(1,5\text{-COD})Ir{\cdot}P_2W_{15}Nb_3O_{62}^{8-}$, Figure 1. This custom-designed polyoxoanion and its supported organometallic complex serve as an effective catalyst precursor to the only *bona fide* polyoxoanion-supported catalyst presently known.[5-8] The most significant features of the present work are the detailed assignments made

[†] Permanent address: Dipartimento di Scienze e Tecnologie Chimiche, Università di Udine, via Cotonificio 108, Udine, Italy.

[‡] Current Address: Department of Chemistry, Colorado State University, Ft. Collins, CO 80523.

[⊗] Abstract published in *Advance ACS Abstracts*, November 1, 1993.

(1) (a) Pope, M. T. *Heteropoly and Isopoly Oxometalates*; Springer-Verlag: Berlin, 1983. (b) Pope, M. T.; Müller, A. *Angew. Chem.* **1991**, *103*, 56.

(2) For instance see: (a) Edlund, D. J.; Saxton, R. J.; Lyon, D. K; Finke, R. G. *Organometallics* **1988**, *7*, 1692. (b) Finke, R. G.; Rapko, B.; Domaille, P. J. *Organometallics* **1986**, *5*, 175. (c) Finke, R. G.; Droege, M. W. *J. Am. Chem. Soc.* **1984**, *106*, 7274. Droege, M. W. Ph.D. Dissertation, University of Oregon, 1984. Rapko, B. Ph.D. Dissertation, University of Oregon, 1986. (d) Pohl, M.; Finke, R. G. *Organometallics* **1993**, *12*, 1453. (e) Rong, C.; Pope, M. T. *J. Am. Chem. Soc.* **1992**, *114*, 2932 and earlier paper in this series. (f) Faraj, M.; Hill, C. L. *J. Chem. Soc., Chem. Commun.* **1987**, 1487. Hill, C. L.; Brown, R. B., Jr. *J. Am. Chem. Soc.* **1986**, *108*, 536. (g) The polyoxoanion complex "$[(C_6H_{13})N]_5[Ru^{III}SiW_{11}O_{39}]$" has been reported but its purity and thus overall composition has been questioned:[2h] Neumann, R.; Abu-Gnim, C. *J. Am. Chem. Soc.* **1990**, *112*, 6025. (h) Randall, W. G.; Weakley, T. J. R.; Finke, R. G. *Inorg. Chem.* **1993**, *32*, 1068.

(3) (a) Finke, R. G.; Droege, M. W.; Cook, J. C.; Suslick, K. S. *J. Am. Chem. Soc.* **1984**, *106*, 5750. (b) Suslick, K. S.; Cook, J. C.; Rapko, B.; Droege, M. W.; Finke, R. G. *Inorg.Chem.* **1986**, *25*, 241.

(4) Since our report of FAB-MS of polyoxoanions, the first mass spectra of any polyoxoanions, others have further demonstrated the usefulness of this technique: (a) Wasfi, S. H.; Costello, C. E. *Synth. React. Inorg. Met.-Org. Chem.* **1989**, *19* (10), 1059. (b) Especially noteworthy is the demonstration of the use of tandem mass spectroscopy [i.e., collision-induced-decomposition (CID) MS/MS] for the characterization of the fragmentation pathways of large inorganic molecules: Wasfi, S. H.; Costello, C. E.; Reingold, A. L.; Haggerty, B. S. *Inorg. Chem.* **1991**, *30*, 1788. (c) Abrams, M. J.; Costello, C. E.; Shaikh, S. N.; Zubieta, J. *Inorg. Chim. Acta* **1991**, *180*, 9–11. (d) Liu, J.; Ortega, F.; Sethuraman, P.; Katsoulis, D. E.; Costello, C. E.; Pope, M. T. *J. Chem. Soc., Dalton Trans.* **1992**, 1901.

0020-1669/93/1332-6034$04.00/0

of a polyoxoanion mass spectrum (the most complete to date), the detailed analysis of the fragmentation pattern of the negative ion mass spectrum (see also the work of Costello, Wafsi, and co-workers[4a-c]), and the comparison of the features and varying value of positive vs negative ion spectra. Overall, the present work provides an illustrative example of the type of information possible from, and the strengths and limitations to, the use of FAB-MS[9] to characterize large, involatile, inorganic complexes.

Experimental Sections

Materials. The synthesis of $[Bu_4N]_9P_2W_{15}Nb_3O_{62}$, **1**,[10] and of its iridium derivative[5,6,10b] $[Bu_4N]_5Na_3[(1,5\text{-COD})Ir{\cdot}P_2W_{15}Nb_3O_{62}]$, **2**, are described in separate publications as indicated. Briefly, the $[Bu_4N]_9P_2W_{15}Nb_3O_{62}$ is prepared by reaction of Nb^V/H_2O_2 with the lacunary ion $[P_2W_{15}O_{56}]^{12-}$. Following a reductive workup and several reprecipitation/purification steps, the intermediate $[(Bu_4N)]_{12}H_4[Nb_6P_4W_{30}O_{123}]$ is isolated. Treatment of this Nb–O–Nb bridged, "dimeric" form with $Bu_4N^+OH^-$ yields the desired, CH_3CN-soluble $[Bu_4N]_9P_2W_{15}Nb_3O_{62}$, **1**. This triniobium-substituted Dawson type anion undergoes reaction with $[Ir(1,5\text{-COD})(CH_3CN)_2]^+$ in CH_3CN in an O_2-free atmosphere to form the polyoxoanion-supported iridium complex $[Bu_4N]_5Na_3[(1,5\text{-COD})Ir{\cdot}P_2W_{15}Nb_3O_{62})]$, **2**, as its mixed Bu_4N^+/Na^+ salt following appropiate cation manipulation steps.[5,6,10b] In addition to the FAB-MS reported herein, the catalyst precursor **2** has been characterized by ^{31}P, ^{183}W, ^{17}O NMR, IR, elemental analysis, and solution molecular weight measurements.[2d,5]

FAB Mass Spectrometry. The compounds were analyzed at Oregon State University by fast atom bombardment mass spectrometry (FAB-MS) in positive ion and negative ion mode. It proved most successful to dissolve the solid powders directly in the FAB matrices on the stainless steel probe. The matrix was dithiothreitol:dithioerythritol (5:1). Most analyses were carried out at mass resolutions of 1000, using raw data (integrated multichannel averaging) or centroided data collection on a Kratos MS-50 mass spectrometer. Some of the spectra were acquired at mass resolution of 4000. Scan rates were 30 or 100 s/decade. Xenon gas was used to generate the primary ionizing beam from an Ion-Tech FAB gun operated at 7–8 keV. Molecular weights and isotope abundance patterns were calculated using the Kratos DS-90 software.

Results and Discussion

Positive Ion FAB-MS of $[Bu_4N]_9P_2W_{15}Nb_3O_{62}$. Figure 2 shows the low resolution (1:1000) positive ion spectrum of $[Bu_4N]_9P_2W_{15}Nb_3O_{62}$. There are two distinct signals: the multicomponent region with peaks clustered around m/z = 5500–6000, and the less intense signal centered around m/z = 11 000. The peaks in the lower, m/z = 5000–6000 mass region consist of five strong signals plus other weaker signals. A parent peak is seen for $[Bu_4N]_9H[P_2W_{15}Nb_3O_{62}]^+$ at m/z = 6273, the result of the addition of a H^+ to the parent compound (H^+ is generated in the dithiothreitol matrix by the FAB process[11]). Three more (four total) of the stronger intensity peaks in the positive-ion FAB-MS in Figure 2 can be accounted for by the precedented[3,4] cation-exchange process between Bu_4N^+ (m/z = 242) and H^+, leading to peaks corresponding to $[Bu_4N]_{9-y}H_{1+y}[P_2W_{15}Nb_3O_{62}]^+$ (y = 1–3; peaks B, D, and F in Figure 2 and Table I). Higher degrees of protonation ($y > 3$) do not give rise to strong intensity peaks due to the loss of oxygen (m/z = 16) as water to form oxygen deficient species such as $[Bu_4N]_{8-y}H_y[P_2W_{15}Nb_3O_{61}]^+$ (y = 0, 1) or $[Bu_4N]_6[P_2W_{15}Nb_3O_{60}]^+$, peaks C, E, and G in Figure 2 and Table I. A general formula accounting for all the assigned peaks in the positive ion FAB-MS in Figure 2 is $[(Bu_4N)_xH_yP_2W_{15}Nb_3O_{62-z}]^+$ (x = 6–9, y = 0–4, z = 0–2). The highest intensity (base) peak at m/z = 5513 is assigned to $[(Bu_4N)_6P_2W_{15}Nb_3O_{60}]^+$.

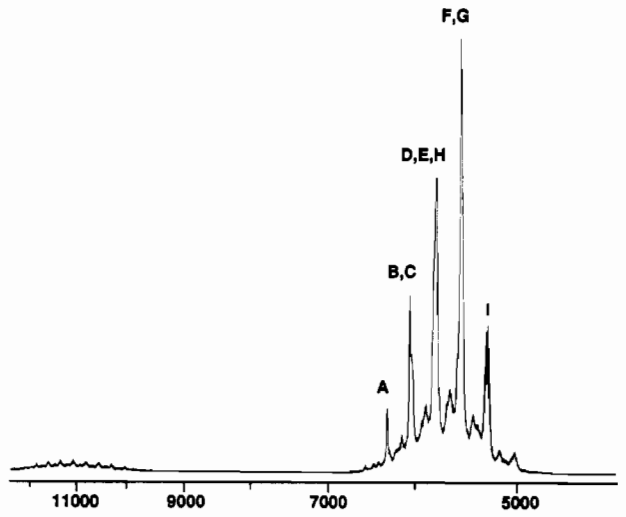

Figure 2. Low-resolution (1:1000) positive FAB mass spectrum of $[Bu_4N]_9P_2W_{15}Nb_3O_{62}$. (For peak assignments, see Table I). This, and all subsequent mass spectral figures herein, exhibit the relative abundance (y-axis) vs m/z (x-axis).

Loss of WO_3 (m/z = 232) and O/H_2O (m/z = 16–18) are the other dominant features here as well as in the other polyoxotungstate FAB mass spectra we[3] and others[4] have seen to date. It should be noted that it is very difficult to unequivocally differentiate the loss of Bu_4N^+ from the loss of WO_3 owing to the small, ca. 10 amu, mass difference between WO_3 (m/z = 232) and Bu_4N^+ (m/z = 242), a mass difference smaller than the natural envelope width of about 15 mass units for this particular size and composition of polyoxoanion.[12] The effect of the simultaneous loss of different fragments would be a slight peak broadening in comparison to the the calculated isotope

(5) (a) Finke, R. G.; Lyon, D .K.; Nomiya, K.; Sur, S.; Mizuno, N. *Inorg. Chem.* **1990**, *29*, 1784. (b) Lyon, D. K.; Mizuno, N.; Nomiya, K.; Pohl, M.; Finke, R. G. Manuscript in preparation. (c) Finke, R. G. In *Polyoxometalates: From Platonic Solids to Anti-Retroviral Activity*; Proceedings of the July 15–17, 1992, Meeting at the Center for Interdisciplinary Research, Bielefeld, Germany; Müller, A., Pope, M. T., Eds.; Kluwer Publishers: Dordrecht, The Netherlands, 1993.

(6) Oxidative catalysis beginning with $(1,5\text{-COD})Ir{\cdot}P_2W_{15}Nb_3O_{62}^{8-}$: (a) Mizuno, N.; Lyon, D. K.; Finke, R. G. *J. Catal.* **1991**, *128*, 84. (b) Trovarelli, A.; Lin, Y.; Finke, R. G. Manuscript in preparation.

(7) Under H_2, in contrast to the situation under O_2 where the Ir remains supported on a single polyoxoanion,[6] we now have good evidence that the Ir–polyoxoanion bonds are cleaved and that $(Ir)_x^{z-}$ nanoclusters are formed: Lin, Y.; Lyon, D. K.; Finke, R. G. Unpublished results.

(8) Interested readers can consult the discussion available elsewhere[5,6] on the significance and strengths (as well as the limitations) of the new class of catalyst materials represented by polyoxoanion-supported catalysts.

(9) FAB-MS has also proven especially useful in determining the composition of large metal cluster compounds: Miller, J. C. *Mass Spectrom. Rev.* **1990**, *9*, 319. Bruce, M. I.; Liddell, M. J. *Appl. Organomet. Chem.* **1987**, *1*, 191. Henly, T. J.; Shapley, J. R.; Rheingold, S. J.; Geib, S. J. *Organometallics* **1988**, *7*, 441. Hayward, C. T.; Shapley, J. R. *Organometallics* **1988**, *7*, 448. Boyle, P. D.; Johnson, B. J.; Alexander, B. D.; Casalnuovo, J. A.; Gannon, P. R.; Johnson, S. M.; Larka, E. A.; Mueting, A. M.; Pignolet, L. H. *Inorg. Chem.* **1987**, *26*, 1346. Hegetschweiler, K.; Keller, T.; Aurein, W.; Schneider, W. *Inorg. Chem.* **1991**, *30*, 873. Anderson, H. L.; Sanders, J. K. M. *J. Chem. Soc., Chem. Commun.* **1992**, 946. Bruce, M. I.; Liddell, M. J. *Inorg. Chim. Acta* **1992**, *198*, 407. Other mass spectrometry techniques (such as ^{252}Cf plasma desorption mass spectrometry) have also been used to investigate large metal clusters: Fackler, J. P.; McNeal, C. J.; Winpenny, R. E. P.; Pignolet, L. H. *J. Am. Chem. Soc.* **1989**, *111*, 6434.

(10) (a) Edlund, D. J.; Saxton, R. J.; Lyon, D. K.; Finke, R. G. *Organometallics* **1988**, *7*, 1692. (b) Mizuno, N.; Lyon, D. K.; Nomiya, K.; Finke, R. G. *Inorg. Synth.*, submitted for publication. (c) See also ref 2d.

(11) Clayton, C.; Wakefield, A. J. C. *J. Chem. Soc., Chem. Commun.* **1984**, 986.

(12) Recall that W has five different naturally abundant isotopes (^{180}W, 0.14%; ^{182}W, 26.41%; ^{183}W, 14.4%; ^{184}W, 30.6%; ^{186}W, 28.41%). As more fully discussed elsewhere,[13] one must remember that the *calculated most abundant mass* ion is not the same as the *monoisotopic mass* ion and is also different from the *average mass*. For example, $P_2W_{15}Nb_3O_{58}^-$ has a calculated most abundant mass of m/z = 4024.6, a monoisotopic mass of m/z = 4027.6 and an average mass of m/z = 4026.4. Due to this natural isotopic distribution, the calculated isotope pattern for most W containing fragments shows that several peaks have almost the same abundance, close to that of the main peak (Table II). This results in further uncertainty in peak assignment (i.e. over and above that in distinguishing the loss of WO_3 vs Bu_4N^+, an uncertainty especially evident at lower resolution).

Table I. Main Peak Assignments (m/z) for Positive and Negative Ion FAB-MS of $[Bu_4N]_{12}P_2W_{15}Nb_3O_{62}$, Arranged According to Decreasing Mass,[a] with a Comparison between Calculated and Experimental Values

fragment	most abundant mass (calcd)	most abundant mass (exptl)	peak labels
$H(Bu_4N)_9P_2W_{15}Nb_3O_{62}^+$	6273	6273	A
$H_2(Bu_4N)_8P_2W_{15}Nb_3O_{62}^+$	6032	6032	B
$(Bu_4N)_8P_2W_{15}Nb_3O_{61}^+$	6014	6015	C (shoulder)
$H_3(Bu_4N)_7P_2W_{15}Nb_3O_{62}^+$	5791	5789	D
$H(Bu_4N)_7P_2W_{15}Nb_3O_{61}^+$	5773	5771	E
$H_4(Bu_4N)_6P_2W_{15}Nb_3O_{62}^+$	5549	5548	F (shoulder)
$(Bu_4N)_6P_2W_{15}Nb_3O_{60}^+$	5513	5512	G
$H(Bu_4N)_7P_2W_{15}Nb_3O_{60}^+$	5757	5757	H
$H(Bu_4N)_5P_2W_{15}Nb_3O_{59}^+$	5256	5254	I
$H(Bu_4N)_7P_2W_{15}Nb_3O_{62}^-$	5789	5787	A′
$H_2(Bu_4N)_6P_2W_{15}Nb_3O_{62}^-$	5547	5547	B′
$H_3(Bu_4N)_5P_2W_{15}Nb_3O_{62}^-$	5305	5305	C′
$H(Bu_4N)_5P_2W_{15}Nb_3O_{61}^-$	5287	5285	D′
$H(Bu_4N)_5P_2W_{15}Nb_3O_{60}^-$	5271	5271	E′
$(Bu_4N)_4P_2W_{15}Nb_3O_{60}^-$	5028	5029	F′
$H(Bu_4N)_3P_2W_{15}Nb_3O_{60}^-$	4787	4786	G′
$H(Bu_4N)_3P_2W_{15}Nb_3O_{59}^-$	4771	4771	H′
$(Bu_4N)_2P_2W_{15}Nb_3O_{59}^-$	4525	4527	I′
$H(Bu_4N)P_2W_{15}Nb_3O_{59}^-$	4288	4287	J′
$H(Bu_4N)P_2W_{15}Nb_3O_{58}^-$	4272	4271	K′
$P_2W_{15}Nb_3O_{58}^-$	4025	4026	L′
$H_2P_2W_{15}Nb_3O_{57}^-$	4010	4013	M′
$P_2W_{14}Nb_3O_{55}^-$	3795	3794	N′
$P_2W_{13}Nb_3O_{52}^-$	3563	3563	O′
$P_2W_{12}Nb_3O_{49}^-$	3329	3330	P′
$H_2(Bu_4N)P_2W_{11}Nb_2O_{45}^-$	3235	3234	Q′
$H_2(Bu_4N)P_2W_{10}Nb_2O_{42}^-$	3002	3002	R′
$H(Bu_4N)P_2W_9Nb_3O_{41}^-$	2894	2894	S′
$(Bu_4N)P_2W_8Nb_4O_{40}^-$	2787	2787	T′

[a] The calculated most abundant masses have been approximated to the nearest unit mass.

Table II. Calculated Isotope Distributions (to $m/z = \pm 0.1$) for Two Fragments Containing W[a]

$P_2W_{15}Nb_3O_{58}$		$[(Bu_4N)_4P_2W_{15}Nb_3O_{60}]$	
mass	%	mass	%
4018.6	1.33	5020.8	1.73
4019.6	3.29	5021.8	1.89
4020.6	4.93	5022.8	3.01
4021.6	5.77	5023.8	9.09
4022.6	8	5024.8	6.69
4023.6	8.17	5025.8	10.29
4024.6	10.11	5026.8	10.38
4025.6	8.96	5027.8	11.07
4026.6	9.51	5028.8	10.43
4027.6	6	5029.8	10.22
4028.6	9.79	5030.8	8.06
4029.6	6.41	5031.8	7.48
4030.6	7.42	5032.8	3.77
4031.6	4.1	5033.8	3.38
4032.6	3.27	5034.8	1.50
4033.6	1.63		
4034.6	1.32		

[a] See footnote 12 for details.

pattern (or even the appearence of shoulders), as we indeed observe (Figure 3). (Some uncertainties in peak assignments are, of course, inherent to the use of FAB-MS with very high molecular weight materials like these.[12,13]) The mass assignments herein have been made using the m/z value at the maximum of the peaks. The good agreement between this value and the calculated *most abundant mass*[13] of the various fragments, Table I, provides convincing evidence that cation-exchange processes involving the loss of Bu_4N^+, concurrent with the addition of H^+, is much more common than the loss of WO_3 fragments (not at all unexpectedly,

(13) For an excellent discussion of these points, with additional examples from organic polymer chemistry, see: Yergey, J.; Heller, D.; Hansen, G.; Cotter, R. J.; Fenselau, C. *Anal. Chem.* **1983**, *55*, 353.

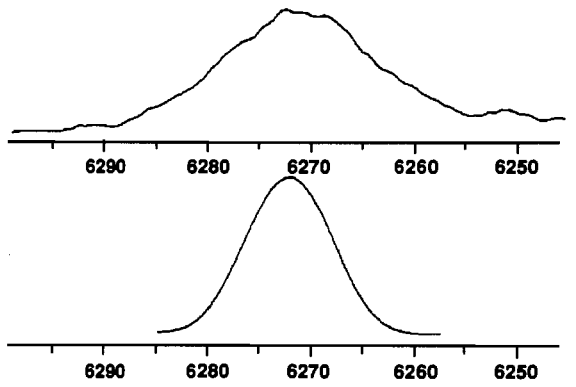

Figure 3. Low-resolution (1:1000) positive FAB mass spectrum of $(Bu_4N)_9P_2W_{15}Nb_3O_{62}$: Experimental (top) and calculated (bottom) molecular ion distributions for $[(Bu_4N)_9HP_2W_{15}Nb_3O_{62}]^+$. The extra broadening seen in the experimental envelope is explained in the text.

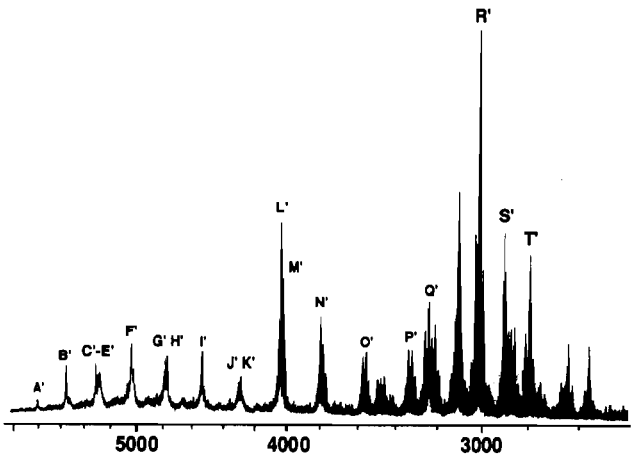

Figure 4. High-resolution (1:4000) negative FAB spectrum of $(Bu_4N)_9P_2W_{15}Nb_3O_{62}$. (For peak assignments, see Table I.)

since WO_3 loss, but not cationization, involves the breaking and restructuring of strong, mixed covalent–ionic W–O and Nb–O bonds).

The detection of peaks at higher m/z values (10 500–11 500) indicates the presence of a small but detectable amounts of the "dimer-like" aggregate $[Bu_4N]_{12}H_4[P_4W_{30}Nb_6O_{123}]$ (m/z = 11 078.45), an intermediate in the preparation of **1**.[10a] It is unclear if this aggregate is present in the original mixture or if it has been formed during the FAB-MS due to the known formation of H^+ in the matrix followed by the well-established H_2O loss reaction (ignoring the non-H^+ cations) to form a Nb–O–Nb bridged species,[10a,14] $2H_xP_2W_{15}Nb_3O_{62}^{x-9} \rightarrow H_2O + H_{2x-2}P_4W_{30}Nb_6O_{123}^{2x-18}$. However, a positive ion spectra of the Nb–O–Nb bridged "dimer-like" agregate $[Bu_4N]_{12}H_4[Nb_6P_4W_{30}O_{123}]$ shows that the *inverse process* (monomer formation from Nb–O–Nb bridge cleavage) can also occur.[2a] This "monomer/dimer" ambiguity is a more general problem in the FAB-MS of polyoxoanions;[4d] hence, caution seems appropriate in using FAB-MS to distinguish dimers from monomers until more examples and data become available.

Negative Ion FAB-MS of $[Bu_4N]_9P_2W_{15}Nb_3O_{62}$. General Features. The negative ion FAB-MS differs significantly from the positive ion FAB-MS in that the high-resolution (1:4000) negative ion FAB of $[Bu_4N]_9P_2W_{15}Nb_3O_{62}$, Figure 4, shows no parent ion but exhibits considerably greater fragmentation.[3,4b] For example, a series of more than 15 envelopes are observed in the mass range from m/z = 6000 to m/z = 2000. A careful and detailed assignment of the peaks has been performed (see Table I), revealing a surprisingly straightforward assigment and showing

(14) Besecker, C. J.; Day, V. W.; Klemperer, W. G.; Thompson, M. R. *J. Am. Chem. Soc.* **1984**, *106*, 4125.

Scheme I. Cation Exchange of H^+ for Bu_4N^+ Followed by H_2O Loss, Accounting for Most of the Observed Fragmentation Processes in the Negative Ion FAB-MS of $P_2W_{15}Nb_3O_{62}^{9-}$

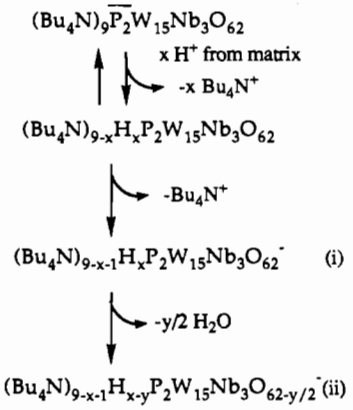

Scheme II. Postulated Mechanism[11] of Electron Capture Followed by H· Abstraction To Account for Species Such as $H(Bu_4N)_5P_2W_{15}Nb_3O_{60}^-$.

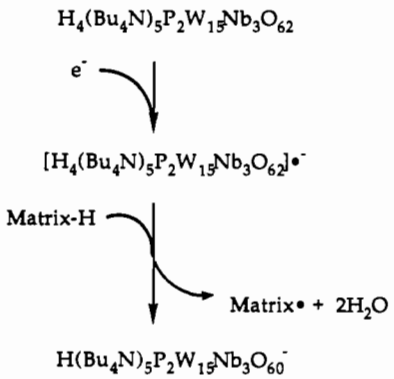

that the peaks in the region m/z = 4000–6000 are formed mainly by the loss of Bu_4N^+ and O from the polyoxoanion.

The most intense envelope in this region occurs at m/z = 4026, which corresponds to $P_2W_{15}Nb_3O_{58}^-$. Replacement of Bu_4N^+ with H^+, with subsequent dissociation and dehydration, explains most of the fragmentation process and also explains the formation of oxygen deficient ions, Scheme I. Both type i and ii fragments (Scheme I) are observed, with type i fragments accounting for ions A′, B′, and C′ in Table I and type ii fragments accounting for ions D′, F′, G′, I′, J′, and L′ in Figure 4 and Table I.

It is also possible to account for other, initially puzzling ions such as $H(Bu_4N)_5P_2W_{15}Nb_3O_{60}^-$. Ions such as these can be explained[11] by electron capture, then hydrogen abstraction from the matrix by the resultant radical, and finally the loss of water, Scheme II. Analogous processes can account for ions E′, H′, K′, and M′ in Figure 4 and Table I. Last, the mass region below m/z 4000 is dominated by the loss of WO_3 fragments;[3,4b,c] this results in the peaks clustered at m/z = 3794, 3563, 3330, and 3234 (peaks N′, O′, P′, and Q′ in Figure 4 and Table I) and other peaks, some of which will be analyzed in detail next.

Identification of "P_2W_{12} Type" Fragments. The most intense base peak in the negative ion FAB mass spectrum of $(Bu_4N)_9P_2W_{15}Nb_3O_{62}$ is at m/z = 3002. Because of the apparently high relative stability of this species, we decided to analyze the m/z = 3002 peak in as great a detail as possible. We were especially interested in the previously unanswered question "do such base peaks in polyoxoanion FAB-MS correspond to a known, stable polyoxoanion solution species?" (If so, then the implication is that negative ion FAB-MS of polyoxoanions could possibly be used as a rapid way to survey for new species which might then be worthy of synthesis and attempts at their isolation.)

Detailed simulations of this m/z = 3002 peak for a series of

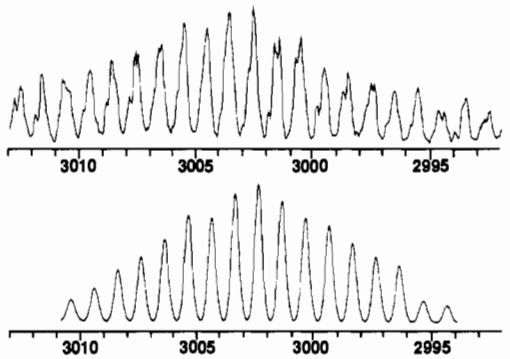

Figure 5. High-resolution (1:4000) negative FAB spectrum of $(Bu_4N)_9P_2W_{15}Nb_3O_{62}$ showing the good agreement between the measured and calculated molecular isotope distributions for the ion $[(Bu_4N)H_2P_2W_{10}Nb_2O_{42}]^-$. The extra splitting in the experimental spectrum is most likely due to the high background (i.e., to the signal-to-noise being somewhat low; we thank a reviewer for a useful discussion of this point vs other possibilities).

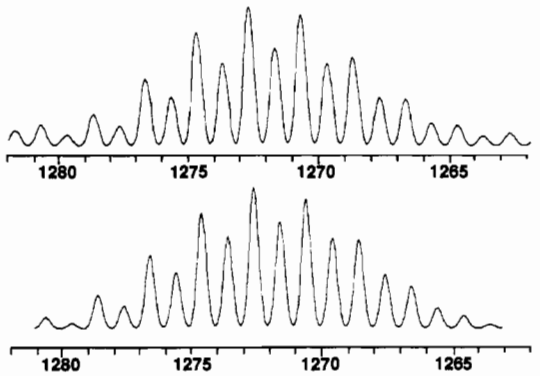

Figure 6. High-resolution (1:4000) negative FAB spectrum of $(Bu_4N)_9P_2W_{15}Nb_3O_{62}$ showing the excellent agreement between measured and calculated molecular ion distributions for the ion $H_4W_5NbO_{16}^-$.

trial-and-error compositions, followed by a visual comparison of the simulations to the observed pattern (at an instrument resolution of m/z = 4000), showed an excellent match between the observed and calculated spectra, revealing that only the composition $H_2(Bu_4N)P_2W_{10}Nb_2O_{42}^-$ fits the structure, Figure 5, top (obsd) and bottom (calculated). A search of the the low-mass region of the negative ion spectrum reveals a peak of composition $H_4W_5NbO_{16}^-$ centered around m/z = 1272; an analogous comparison of the observed spectrum (Figure 6, top) and the calculated one (Figure 6, bottom) again leaves little doubt that the fragment identified has the composition $H_4W_5NbO_{16}^-$. Adding the polyoxoanion component of this fragment onto the $P_2W_{10}Nb_2O_{42}^{4-}$ yields the composition $P_2W_{15}Nb_3O_{58}^-$ (peak L′ in Table I) as a *suggested* precursor to these two fragments.[15]

It is noteworthy that the fragment $H_4W_5NbO_{16}^-$ corresponds to the well-known hexametalate structural type,[16] that is, $W_6O_{19}^{2-}$,[16a] $Nb_6O_{19}^{8-}$,[16b] and even the observed[16c] $W_5NbO_{19}^{3-}$ itself. Similarly, the fragment $H_2(Bu_4N)P_2W_{10}Nb_2O_{42}^-$ has well-established (solution chemistry) precedent in the proposed $H_xP_2W_{12}O_{48}^{(14-x)-}$ composition and structure,[17,18] derived from the Well–Dawson anion $P_2W_{18}O_{62}^{6-}$ by formally removing a six

(15) The fact that no relevant fragments of composition $H_4W_5NbO_{20}^-$ are detected suggests that the main peak at m/z = 3002 (i.e. $H_2(Bu_4N)P_2W_{10}Nb_2O_{42}^-$) is formed by a secondary fragmentation process from $P_2W_{15}Nb_3O_{58}^-$ and not directly from the starting material, $P_2W_{15}Nb_3O_{62}^{9-}$.

(16) (a) Fuchs, J.; Freiwald, W.; Hartl, H. *Acta Crystallogr.* **1978**, *B34*, 1764. (b) Liudqvist, I. *Ark. Kemi* **1952**, *5*, 667. (c) Dabbabi, M.; Boyer, M. *J. Inorg. Nucl. Chem.* **1976**, *38*, 1011.

(17) Contant, R.; Ciabrini, J. P. *J. Chem. Res.* (*S*) **1977**, 222; *J. Chem. Res.* (*M*) 2601. Contant, R.; Ciabrini, J. P. *J. Inorg. Nucl. Chem.* **1981**, *43*, 1525.

(18) Acerete, R.; Hammer, C. F.; Baker, L. C. W. *Inorg. Chem.* **1984**, *23*, 1478.

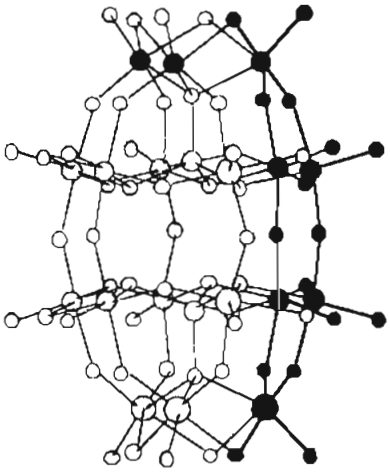

Figure 7. Representation of the Well–Dawson type structure[18] for the parent $P_2W_{15}Nb_3O_{62}^{9-}$ but with the darkened atoms and bonds showing the W_5NbO_{16} fragment lost to yield the known P_2W_{12} structure type.[18,19]

tungsten "W_6O_{14}" group.[18] The most reasonable initial proposal, then, for the structure of the *previously unknown composition* $P_2W_{10}Nb_2O_{42}^{4-}$ is that it is analogous to the structure determined for the "P_2W_{12}" ion by ^{183}W NMR[18] in which the W_6 slice has been removed from the side of the Wells–Dawson $P_2W_{18}O_{62}^{6-}$ structure. In our case the $P_2W_{10}Nb_2O_{42}^{4-}$ framework results by formally "peeling off" an entire $-NbO_2-(O)_2-(W_2O_3-(O)_2-W_2O_3)-(O)_2-WO_2$ group from the side of our $P_2W_{15}Nb_3O_{58}^{-}$ ion (formed from the parent $P_2W_{15}Nb_3O_{62}^{9-}$ by losing four H_2O molecules, Scheme I, peak L′ in Table I), Figure 7. Note that the C_{3v} symmetry of the parent $P_2W_{15}Nb_3O_{62}^{9-}$ means that three different but symmetry (and thus chemically) equivalent "slices" can be removed to yield the same composition fragment. (We *do not* mean to imply this as the explicit or only possible mechanism, but rather use this to emphasize the structural analogy to "P_2W_{12}".) The stability of these "$P_2W_{12-x}Nb_x$" fragments accounts also for the presence of other two intense signals below $m/z = 3000$ (S′ and T′ in Figure 4 and Table I). They have been assigned respectively to $[H(Bu_4N)P_2W_9Nb_3O_{41}]^-$ and $[(Bu_4N)P_2W_8Nb_4O_{40}]^-$ resulting from the base peak (peak R′ in Figure 4 and Table I) by formal replacement of a WO_3 unit with a NbO_2 fragment. Again, the comparison between experimental and calculated patterns shows a good match between experimental and calculated distributions (Figure 8a, b). The comparison of the relative intensities between the calculated and observed spectra in Figure 8b shows some discrepancy observable on the left side of the envelope (m/z = 2788–2796). This small discrepancy is ascribable to the presence of a fairly intense envelope which clusters at about m/z = 2804 and thus affects the relative intensities on the left side of the spectrum. (Alternatively, the presence of a high background signal in that region could account for some of this difference.)

Another point worth noting here is how FAB mass spectra are useful in reliably determining the number of oxygen atoms in a given polyoxoanion framework. In our experience,[19] this is a major step in avoiding misformulated polyoxoanions.

Positive and Negative Ion FAB-MS of the Supported Organometallic Complex (1,5-COD)Ir·$P_2W_{15}Nb_3O_{62}^{8-}$. Figure 9 shows the positive (top) and negative (bottom) ion FAB-MS of the supported organometallic complex $(Bu_4N)_5Na_3(1,5\text{-COD})Ir\cdot P_2W_{15}Nb_3O_{62}$. No parent ion is seen. The introduction of the supported organometallic fragment Ir(1,5-COD)$^+$ and the Na^+ counterions result in a further broadening of the peak envelopes in both the positive and negative spectra; however, identifiable fragments are still present. In the positive ion spectrum, a very

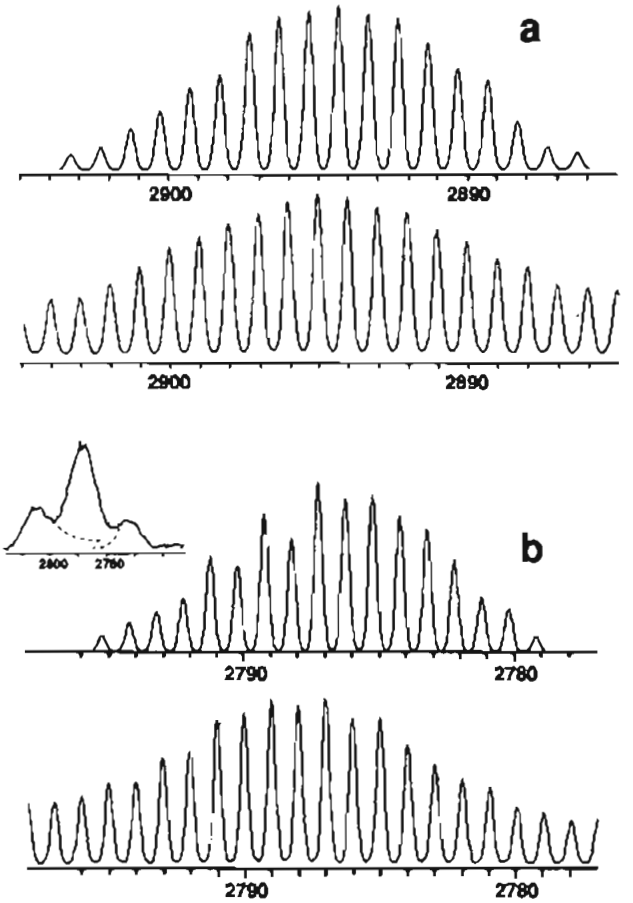

Figure 8. High-resolution (1:4000) negative FAB spectrum of $[Bu_4N]_9P_2W_{15}Nb_3O_{62}$ showing the good agreement between simulated and measured molecular ion distribution for (a) $H(Bu_4N)P_2W_9Nb_3O_{41}^-$ and (b) $(Bu_4N)P_2W_8Nb_4O_{40}^-$. In the inset is shown a part of the low-resolution negative FAB spectrum of $(Bu_4N)_9P_2W_{15}Nb_3O_{62}$ in the region m/z 2810–2760 (see the text for details).

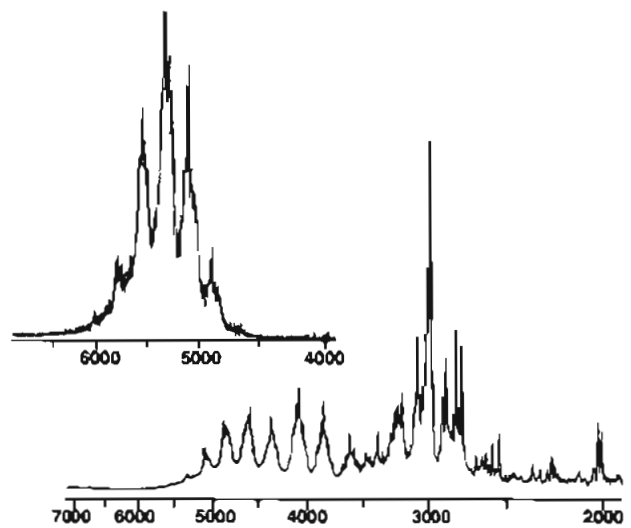

Figure 9. Low-resolution (1:1000) (a) positive and (b) negative ion spectra of $(Bu_4N)_5Na_3[(1,5\text{-COD})Ir\cdot P_2W_{15}Nb_3O_{62}]$.

broad signal from ca. m/z = 4500 to 6500 and containing three major envelopes is observed. The main peak in the central envelope at m/z = 5373 can be assigned to the ion resulting from loss of the organometallic Ir(1,5-COD)$^+$ moiety, that is to $[(Bu_4N)_5Na_3H_2P_2W_{15}Nb_3O_{62}]^+$. Presumably, it is the e^- or H^+ (or both) generated by the FAB of the dithiothreitol matrix which cause the loss of the Ir(1,5-COD)$^+$ moiety. The other two most intense envelopes cluster around m/z = 5590 and 5150; these result from exchange processes involving Na^+, Bu_4N^+, and H^+ and can be

(19) Finke, R. G.; Droege, M. W. *Inorg. Chem.* **1983**, *22*, 1006.

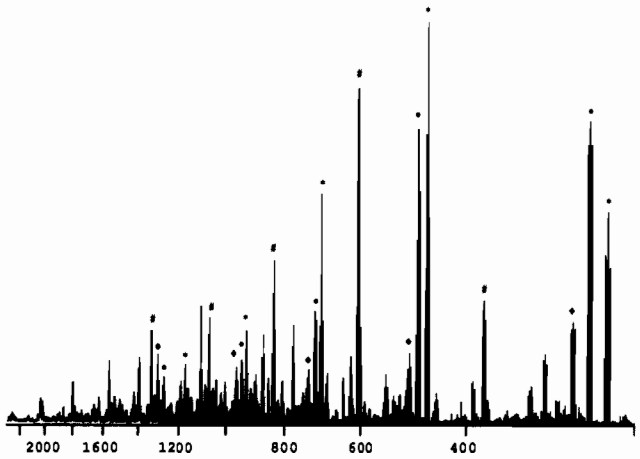

Figure 10. High-resolution (1:4000) negative spectrum of $(Bu_4N)_9P_2W_{15}Nb_3O_{62}$ showing details of the low-mass region. *, $(WO_3)_n$, ●, $HO(WO_3)_n$, ♦, $HO_2(WO_3)_n$, #, $NbO_3(WO_3)_n$ (n = 1–5).

assigned to $[(Bu_4N)_6Na_2H_2P_2W_{15}Nb_3O_{62}]^+$ and $[(Bu_4N)_4Na_4H_2P_2W_{15}Nb_3O_{62}]^+$, respectively. The loss of O plus Na^+ exchange provides a plausible explanation for the broadening of each peak in the envelopes (20–30 m/z units).

The negative ion FAB-MS spectrum of $(Bu_4N)_5Na_3[(1,5\text{-COD})Ir{\cdot}P_2W_{15}Nb_3O_{62}]$ again shows more fragmentation (i.e. as was observed in a comparison of the positive and negative ion spectra for the parent polyoxoanion, $(Bu_4N)_9P_2W_{15}Nb_3O_{62}$). At least 10 envelopes of peaks are observed in the range from m/z = 5150 to 2800. The first cluster at around m/z = 5120 can be assigned to $(Bu_4N)_4Na_4P_2W_{15}Nb_3O_{62}^-$; hence, the loss of Ir(1,5-COD) (i.e. $Ir(1,5\text{-COD})^+ + e^-$) and exchange between Bu_4N^+ and Na^+ ions have again occurred. All the other envelopes result from exchange process and loss of WO_3 fragments (e.g. the peak at m/z = 3002 discussed in detail previously). The expected loss of oxygen cannot be detected due to broadness of the observed peaks.

Some interesting differences in the negative ion mass spectrum of $(Bu_4N)_5Na_3[(1,5\text{-COD})Ir{\cdot}P_2W_{15}Nb_3O_{62}]$ vs that of the parent $[(Bu_4N)_9P_2W_{15}Nb_3O_{62}]$ are worth mentioning. One is the lack of a peak at m/z 4026 due to $P_2W_{15}Nb_3O_{58}^-$; a reasonable explanation for this is that the presence of Na^+ ions decreases the probability of formation of a totally H^+-exchanged anion[3,4b] like $H_8P_2W_{15}Nb_3O_{62}^-$ that is prone to complete dehydration to $P_2W_{15}Nb_3O_{58}^-$ (with a presumed increase in the probability of *mixed salts* of general formula $(Bu_4N)_xNa_yH_zP_2W_{15}Nb_3O_{62}$ that are apparently less prone to dehydration). The other different feature is the presence of broader envelopes in the negative ion spectrum of the supported organometallic. This is due to the presence of Na^+ which increases the probability of formation of mixed fragments of the type $(Bu_4N)_xNa_yH_z[P_2W_{15}Nb_3O_{62}]$. *The implication here is that fully cation-exchanged free acid salts such as "$H_9P_2W_{15}Nb_3O_{62}$" may be among the most valuable for FAB-MS characterization studies.*

Analysis of the Low-Mass Region of the Spectra. A further piece of evidence in support of the general fragmentation patterns proposed comes from the analysis of the low-mass region of the spectra from m/z 200 to 1400, Figure 10. This region is dominated by the signals from oxide fragments containing W, Nb, or a mixture of the two. For example, $(WO_3)_n$, $HO(WO_3)_n$, $HO_2(WO_3)_n$, and $NbO_3(WO_3)_n$ (n = 1–5) have been identified as shown by the assignments indicated in Figure 10, accounting for 20 envelopes from m/z 232 to 1301. All of these peaks correspond to different parts of the "slice" from $P_2W_{15}Nb_3O_{62}^{9-}$ as depicted in Figure 7. Interestingly, no fragments containing two Nb atoms have been detected indicating that bond breaking in the direction perpendicular to that of the main fragmentation pattern (i.e. along the C_{3v} axes) is not likely to occur. The general features are very similar for both the polyoxoanion and the supported organometallic complex, indicating that this region could be used as a fingerprint for the polyoxoanion skeleton $P_2W_{15}Nb_3O_{62}^{9-}$. This is also indirect evidence that the $Ir(1,5\text{-COD})^+$ fragment is lost prior to desorption (probably as the neutral fragment "Ir(1,5-COD)•" following electron capture, as no signals due to Ir or COD or a combination of these species have been detected in the low-mass region). Moreover, the close similarity between the fragmentation pattern of **1** and its supported $Ir(1,5\text{-COD})^+$ complex **2** in the low-mass region confirms[5,10] that no change of the polyoxoanion skeleton has occurred following the surface attachment of $Ir(1,5\text{-COD})^+$.

Conclusions

In conclusion, the evidence continues to accumulate that FAB-MS is a rapid and convenient tool for the characterization of massive polyoxoanions and their derivatives.[3,4] The present work extends the use of FAB-MS for the rapid and, in cases like the parent $P_2W_{15}Nb_3O_{62}^{9-}$, the unequivocal compositional characterization of even massive and highly charged polyoxoanions. In addition, it has been demonstrated how most of the observed spectra can be assigned rather quickly (more than 50 peak envelopes have been assigned) and with a great deal of confidence, especially when accompanied by quantitative simulations of key, strong-abundance peaks in the spectrum.

Additional specific points worth summarizing[20] (at least for the present polyoxoanions and probably for many others) are the following: (i) positive ion spectra are more useful for a simple parent ion MW determination; (ii) negative ion spectra give richer fragmentation patterns (and often more intense spectra[4b]); (iii) the fragmentations observed can be readily accounted for by cationization processes ($Bu_4N^+/H^+/Na^+$) and tandem mass spectroscopy verified[4b] WO_3 and O/H_2O loss;[3,4] (iv) the most abundant peaks in at least the present case corresponds to a known, stable fragments from solution chemistry (i.e. the "P_2W_{12}" type fragment "$P_2W_{10}Nb_2$"); (v) high-resolution work needs to consider and avoid sources of multiple peaks and thus peak broadening (by sticking to a single cation type and avoiding mixed cations like Na^+/Bu_4N^+) and to avoid even Bu_4N^+ (if it is important to distinguish fragmentations involving Bu_4N^+ vs WO_3 loss); (vi) the preparation and examination of free acid salts of polyoxoanions (e.g. $H_9P_2W_{15}Nb_3O_{62}$) deserves experimental scrutiny as a possible route to relatively clean and interpretable FAB mass spectra of polyoxoanions; and (vii) finally, a reliable determination of the number of oxygen atoms by FAB-MS can help avoid misformulated polyoxoanions.

It is also important to emphasize the possibility (which clearly emerges from this work plus the work of Costello and co-workers[4]) of rationalizing the FAB-MS spectra of polyoxoanions in terms of simple mechanisms and known chemical considerations. In this regard, inorganic mass spectrometry of polyoxoanions has taken a step closer to a domain that had so far been mainly a prerogative of organic mass spectrometry. Such less empirical and more rational interpretation of the mass spectra of inorganic compounds should enhance the use of this valuable technique in inorganic chemistry.

Acknowledgment. We thank Professor Max Deinzer, Department of Agricultural Chemistry, Oregon State University, Corvallis, OR, for making available to us their Kratos MS 50 mass spectrometer. We are also indebt to Dr. Brian Arbogast for his expert technical assistance in carrying out the FAB-MS measurements and the spectral simulations. This work was supported by the Department of Energy, Chemical Sciences Division, Office of basic Energy, via Grant DOE-DE-FG06-089ER13998.

(20) One other point is that FAB-MS of the supported *mono*cationic organometallics do not yield parent ions, at least in our studies to date. The use of e^- capturing nitroaromatic matrices and H^+ capturing agents (e.g. possibly polyvinylpyridine) are possibilities worthy of additional investigation.